energies

MDPI

Article

Optimization Method for the Evaluation of Convective Heat and Mass Transfer Effective Coefficients and Energy Sources in Drying Processes

Marcin Stasiak [1], Grzegorz Musielak [2,*] and Dominik Mierzwa [2]

[1] Institute of Mathematics, Poznań University of Technology, 60-965 Poznań, Poland; Marcin.Stasiak@put.poznan.pl

[2] Institute of Technology and Chemical Engineering, Poznań University of Technology, 60-965 Poznań, Poland; Dominik.Mierzwa@put.poznan.pl

* Correspondence: Grzegorz.Musielak@put.poznan.pl; Tel.: +48-61-665-3622

Received: 12 November 2020; Accepted: 10 December 2020; Published: 14 December 2020

Abstract: A new optimization method for the assessment of the coefficients existing in a model of drying kinetics is developed and presented in this article. This method consists of matching the drying kinetics resulting from the mathematical model with the drying kinetics resulting from the experiments. Both the heat and mass transfer coefficients, the critical relative humidity, and the additional ultrasound energy (heat) source are included in the optimization procedure. The Adams–Bashforth multistep method of solving nonlinear ordinary differential equations is used. The inverse problem of model parameter estimation is solved by the Rosenbrock optimization method. The methodology is illustrated by the example of the ultrasound-assisted convective drying of apple and carrot. A high level of agreement between the results obtained experimentally and numerically was found. The obtained results confirmed the great influence of ultrasound on the drying kinetics. It was found that ultrasound application improved the mass transfer by 20–80% and heat transfer by 30–90%. It was also found that the heating effect caused by the ultrasound's absorption was very small, with a value below 1%.

Keywords: mass and heat transfer coefficients; heat source; evaluation; ultrasound

1. Introduction

Biological materials require very gentle drying methods because they are extremely sensitive to a high temperature and long process time [1,2]. Simple convection drying often leads to the degradation of these materials. For this reason, hybrid methods which combine convective drying with ultrasound assistance have been developed in recent decades [3]. The results of this development may have a positive effect on the production and storage of fruit and vegetables. In the drying technology of biological products, new drying methods applying ultrasound and microwave enhancement are required [4]. This can significantly reduce the energy consumption, shorten the drying time, and improve the quality of food by preserving its valuable nutrients (proteins, carbohydrates, vitamins, and minerals) and visual aspects (color and shape).

The published literature [5–10] indicates that a high-intensity ultrasound is able to improve the mass and heat transfer processes of dried products. This is especially true for drying materials such as vegetables and fruits, which are biological materials sensitive to high temperatures. The positive attributes of such methods have recently led to an innovative ultrasound apparatus being developed [11]. New investigations and possibilities of ultrasound-assisted drying as a result of new dryer application using ultrasound have been proposed [9,12–16]. A broad review of ultrasound use in drying processes is presented in [3].

To describe ultrasound-assisted drying, a number of drying models enabling the assessment of the drying kinetics and process effectiveness have been developed. The simplest models are the empirical ones, which interpolate experimental data using exponential functions, e.g., the Weibull model [13]. The models of this type allow the effective diffusion coefficient to be determined. Another group of models includes the diffusion ones. Some of these models neglect external resistance [17,18], whilst others consider this resistance [19,20]. These models only describe the mass transfer, and do not describe the heat transfer. A model that describes simultaneous mass and heat transfer and takes into account external resistance is described in [21]. Unfortunately, this model does not account for material shrinkage. This is a drawback, especially when describing drying food. A model taking into account heat and mass transfer, together with external resistance and material shrinkage, has been developed by Kowalski and Pawłowski [10,22]. In our article, this model is used to describe the drying kinetics. Mathematical modeling of the drying process needs to determine the process parameters [23]. To evaluate the drying kinetics according to the model proposed above, it is necessary to determine the model parameters, namely, the effective coefficients of heat h_T and mass h_m transfer, as well as the energy source due to ultrasound absorption ΔQ and the critical moisture content X_{cr}. The main aim of this work is to present a numerical algorithm for the evaluation of these parameters. In modeling and simulations of the heat and mass transfer processes in the available literature, the Runge–Kutta method and ready-made solvers (e.g., implemented in MatLab) are often used [24–26]. This method of the ordinary differential equations solution is not stable for long-term simulation. Therefore, the Adams–Bashforth method was used in this work [27]. The model parameters were estimated on the basis of the ultrasound-assisted drying kinetics realized experimentally. The estimation was based on the inverse problem solution, obtained by the use of optimization techniques. The non-gradient Rosenbrock optimization method was chosen because of its efficiency [28].

2. Mathematical Model

Here, drying is considered as a coupled heat and mass transfer process described by a global model of drying kinetics, that is, a model expressing the variation of the drying material moisture content and temperature over time. The drying kinetics is described by a system of coupled ordinary differential equations [10,22]:

$$m_s \frac{dX}{dt} = -A_m h_m \ln \frac{\varphi|_{\partial B} p_{vs}(T)}{\varphi_a p_{vs}(T_a)}, \tag{1}$$

$$m_s \frac{d}{dt}[(c_s + c_l X)T] = A_T h_T (T_a - T) - A_m l h_m \ln \frac{\varphi|_{\partial B} p_{vs}(T)}{\varphi_a p_{vs}(T_a)} + \Delta Q, \tag{2}$$

where X is the moisture content (dry basis); T denotes the temperature; m_s is the dry mass; A_m and A_T denote the surfaces of mass and heat exchange, respectively; φ_a is the relative air humidity in ambient air; $\varphi\big|_{\partial B}$ is the air humidity close to the dried sample surface; p_{vs} is the temperature-dependent saturated vapor pressure; c_s and c_l denote the specific heat of dry solid and moisture, respectively; l is the latent heat of evaporation; h_m and h_T denote the mass and heat transfer coefficients, respectively; and ΔQ is the heat in the material sample due to the absorption of ultrasonic waves. Both equations are determined as a result of the mass and energy balances. Equation (1) describes the mass exchange: The mass accumulation of moisture (left hand side) is equal to the convective moisture mass flux (right hand side). Equation (2) describes the heat transfer between the dried material and the surrounding air: The heat accumulation (left hand side) is equal to the heat flux delivered by convection (the first term to the right hand side) minus the heat consumed by evaporation (the second term to the right hand side) plus the heat of ultrasonic wave absorption (the third term to the right hand side).

This model of drying kinetics is used to describe the drying of strongly deformable biological materials, such as fruit and vegetables. Therefore, it is necessary to take into account that such materials

undergo a large amount of shrinkage during drying. It is assumed that the dried material undergoes linear volumetric shrinkage according to the following formula:

$$V = V(X) = [1 - \alpha_V(X_0 - X)]V_0, \tag{3}$$

where α_V denotes the volumetric shrinkage coefficient, X_0 is the initial moisture content, and X represents the actual moisture content. The surfaces A_m and A_T (Equations (1) and (2)) denote the surfaces of mass and heat exchange, respectively. If the dried material is placed on a moisture-impermeable support, the surfaces A_m and A_T are different. If, on the other hand, the material experiences constant motion during drying, the evaporation area is not limited. In this case, the heat and mass exchange occurs through the whole material surface. Then, the surfaces A_m and A_T are equal. In the rotary dryer used in our tests (Figure 1), the material is not supported and experiences constant motion, and both heating and drying take place over the whole surface. Hence, a simple transformation of Equation (3) gives the area of both mass and heat exchange as a function of humidity, described by the following equation:

$$A_m = A_T = A(X) = [1 - \alpha_V(X_0 - X)]^{2/3}A_0. \tag{4}$$

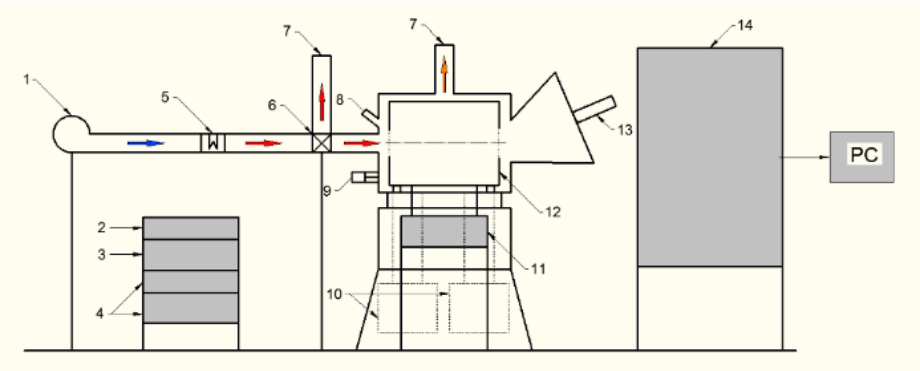

Figure 1. The scheme of the hybrid dryer: 1—blower (fan); 2—AUS controller; 3—AUS preamplifier; 4—microwave feeders; 5—heater; 6—pneumatic valve; 7—air outlet; 8—pyrometer; 9—drum drive; 10—microwave generators; 11—balance; 12—rotatable drum; 13—AUS ultrasound transducer; and 14—control unit.

At the beginning of drying, the material is heated. Then, usually, two periods can be distinguished in the drying chart [29] (see Figure 2a).

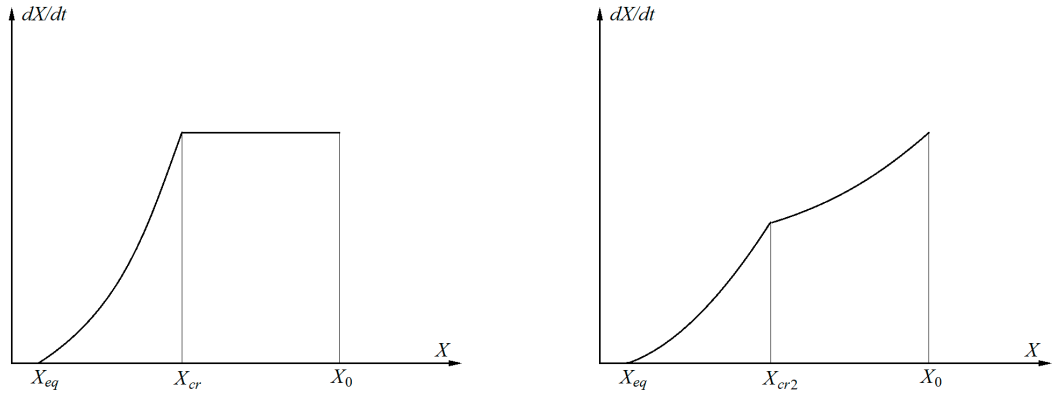

(**a**) (**b**)

Figure 2. Schematic presentation of the drying rate function: (**a**) Existence of the constant drying period, and (**b**) existence of the two stages of the falling drying rate period.

The first one is called the constant drying rate period (CDRP). During this period, a film of free moisture exists on the surface of the dried material. The drying rate only depends on external conditions. During this period, the temperature of the dried material does not change. When the average moisture content reaches its critical value X_{cr}, the free moisture film is reduced and the drying rate decreases. The falling drying rate period (FDRP) starts. During this period, the temperature of the dried material rises to the equilibrium temperature.

The proposed model enables the description of the material heating, the constant (CDRP), and the falling (FDRP) drying rate periods. One of the possibilities for describing the above periods using the mathematical model presented above (Equations (1) and (2)) is the adoption of a discontinuous function describing the dependence of the relative air humidity at the surface of the dried material $\varphi|_{\partial B}$ on the moisture content in the dried material X [30]:

$$\varphi|_{\partial B} = \begin{cases} 1 & \text{for } X_0 \geq X \geq X_{cr} \\ \varphi_a + (1-\varphi_a)\frac{X-X_{eq}}{X_{cr}-X_{eq}} & \text{for } X_{cr} \geq X \geq X_{eq} \\ \varphi_a \frac{X}{X_{eq}} & \text{for } X_{eq} \geq X \end{cases}, \tag{5}$$

where X_0, X_{cr}, and X_{eq} are the initial, critical, and equilibrium values of the moisture contents, respectively and φ_a is the relative humidity of the drying medium. The critical moisture point X_{cr} describes the transition between the constant drying rate period (CDRP) and the falling drying rate period (FDRP).

Based on the experimental tests, one can state that during the drying of fruits and vegetables, no CDRP exists [1]. In some cases, the FDRP period can be divided into two stages [29] (see Figure 2b). The first stage could be interpreted as a result of a decrease in the dried material surface, which causes a decrease in the drying rate. During the second drying stage, the drying rate only depends on the internal mass transfer resistance. To describe these two stages of the FDRP, the following relation is proposed [30]:

$$\varphi|_{\partial B} = \begin{cases} \varphi_{cr2} + (1-\varphi_{cr2})\frac{X-X_{cr2}}{X_0-X_{cr2}} & \text{for } X_0 \geq X \geq X_{cr2} \\ \varphi_a + (\varphi_{cr2}-\varphi_a)\frac{X-X_{eq}}{X_{cr2}-X_{eq}} & \text{for } X_{cr2} \geq X \geq X_{eq} \\ \varphi_a \frac{X}{X_{eq}} & \text{for } X_{eq} \geq X \end{cases}, \tag{6}$$

where the second critical point (X_{cr2}, φ_{cr2}) describes the transition between the two aforementioned stages of the FDRP.

At a constant total pressure (equal to 0.1 MPa) of humid air, the pressure of saturated vapor p_{vs} is a function of temperature:

$$\begin{aligned} p_{vs}(T) = {} & 9.61966 \times 10^{-4} T^4 - 1.08405264 \times T^3 + 4.61325529 \times 10^{-2} T^2 \\ & -8.77803513 \times 10^{-4} T + 6.29588464 \times 10^6, \end{aligned} \tag{7}$$

where T is the absolute temperature ranging between 273 and 373 K. This function is obtained by the interpolation of experimental data presented in [31].

3. Solution Method

The drying kinetics of Equations (1) and (2) should be rearranged to produce the following forms:

$$\frac{dX}{dt} = -\frac{A_m h_m}{m_s} \ln \frac{\varphi|_{\partial B}\, p_{vs}(T)}{\varphi_a p_{vs}(T_a)}, \tag{8}$$

$$\frac{dT}{dt} = \frac{1}{m_s(c_s + c_l X)} \left[A_T h_T (T_a - T) + (c_l T - l) A_m h_m \ln \frac{\varphi|_{\partial B}\, p_{vs}(T)}{\varphi_a p_{vs}(T_a)} + \Delta Q \right]. \tag{9}$$

This transformation allows us to present the initial problem in the form of a system of two nonlinear ordinary differential equations with appropriate initial conditions. This system can be written as

$$\begin{cases} \frac{dX}{dt} = \Psi(t, X, T) \text{ for } t > 0 \\ \frac{dT}{dt} = \Phi(t, X, T) \text{ for } t > 0 \\ X(t=0) = X_0 \; T(t=0) = T_0 \end{cases} . \quad (10)$$

Drying is a long process. Therefore, the solution of the above system of equations requires the use of an appropriate numerical method for such problems. Therefore, the Adams–Bashforth method was used to solve the system of Equation (10) [27]. This is an explicit method of solving nonlinear ordinary differential equations. It is based on Lagrangian polynomial interpolation of the solution. The method is a non-self-starting multistep one. This means that, in order to use this method, four starting points must be specified with another numerical method. These points were obtained using the fourth row Runge–Kutta method [32].

4. Model Parameter Determination

In order to determine the values of the process parameters in the mathematical model, the solution of the inverse problem is used. It consists of searching for the direct problem solution that is closest to the experimental results describing the kinetics of the process. The best fit between the experimental and numerical results is obtained using optimization techniques. Four parameters, which describe the drying process, are introduced in the mathematical model (Equations (1)–(7)): The heat h_T and mass h_m transfer coefficients; the heat source ΔQ describing the absorption of ultrasonic waves; and the critical relative humidity φ_{cr2}.

The optimal numerical solution is sought in the quadratic norm. This means that the best fit occurs when the sum of the squares of the residuals of the experimental and numerical values is the smallest. However, the numerical values of these differences in the moisture content and the temperature are of different orders. Therefore, the differences are normalized by dividing them by their maximum values. As a result, the share of both parameters—the moisture content and the temperature—is of the same order in the objective function which is defined as follows:

$$f(h_m, h_T, \Delta Q, \varphi_{cr2}) = \sum_{i=1}^{N} \left[\left(\frac{X_{\text{num},i} - X_{\text{exp},i}}{X_{\max} - X_{\min}} \right)^2 + \left(\frac{T_{\text{num},i} - T_{\text{exp},i}}{T_{\max} - T_{\min}} \right)^2 \right]. \quad (11)$$

The search for the minimum of the objective function (11) is a four-parameter optimization problem. Calculation of the numerical value of this function does not require a long computation time, but its derivatives in relation to independent variables cannot be determined. Therefore, an appropriate non-gradient optimization method should be used. The Rosenbrock optimization method was chosen as the appropriate one to solve the formulated optimization problem [28].

5. Materials and Methods

The proposed method for determination of the model parameters is illustrated for the ultrasound-assisted convective drying of apple and carrot samples, as examples.

There are two material parameters used in the model, namely, the specific heat of dry solid c_s and the volumetric shrinkage coefficient α_V. Their values should be determined before starting the optimization procedure. The value of the material specific heat c_s as a function of temperature was calculated based on formulas described in the literature [33]. The procedure employed for calculating the specific heat of the moist material was as follows. First, the mass fractions of the components contained in the apples and carrots were determined on the basis on the data from the National Food Institute of the Technical University of Denmark [34]. The individual specific heats of all constituents

as temperature functions (polynomials) were determined on the basis of [33]. Then, the specific heat of dry matter was obtained as the sum of the products of the individual specific heats and the mass fractions of the components. The specific heat of the wet material is the sum of the specific heat of dry matter and the specific heat of water (temperature-dependent) multiplied by the moisture content X (see Equation (2)). The volumetric shrinkage coefficient, α_V, was determined on the basis of an additional set of experiments. During the experiments, the materials were subject to slow convection drying. The volumes of fresh material samples were measured before drying and in given time intervals during the process. The measurement was carried out with the use of the gravimetrical method based on Archimedes' law. In this method, the volume is calculated on the basis of weight measurement in air and water. Due to the amount of water removed by the sample, its weight in water is less than in air. The weight difference enables the sample volume measurement.

The drying kinetics was determined from the experimental tests carried out in the rotary hybrid dryer, which allows drying with three different techniques, i.e., hot air, microwaves, and ultrasound used separately and/or simultaneously. Microwaves were not used during these experiments. The scheme of the dryer is shown in Figure 1.

The material under first investigation was an apple (*Malus domestica* cv. Ligol), bought at a local market and stored in a refrigerator at a temperature of 5 °C prior to the experiments. For each test, fresh fruits were cut into 10 mm size cubes, and 200 g of such material was taken for drying experiments. The second material under investigation was a carrot (*Daucus carota* L. cv. Nantes), bought at the same place and stored in the same way as apples. The vegetable portion used for drying tests had a similar shape to the previous one. For each test, fresh carrots were cleaned and cut into slices with a 5 mm thickness. The amount of material taken for drying experiments was equal to 200 g. All of the tests were carried out according to the schemes and process parameters listed in Table 1. The air velocity was controlled by the flow sensor placed in the pipeline between the fan and the drying chamber. The diameters of the pipe and the drying chamber were different, so the effective air velocity in the chamber was five times smaller than the velocity in the pipe. The values of both velocities are described in Table 1.

Table 1. Drying schemes and parameters.

Scheme No. and Abbreviation	Convective Drying Parameters	Ultrasound Power If Used
Apples		
1—CV_404	40 °C, air flow 4 m/s (effective 0.8 m/s)	–
2—CVUD_404200	40 °C, air flow 4 m/s (effective 0.8 m/s)	200 W
Carrots		
1—CV_502	50 °C, air flow 2 m/s (effective 0.4 m/s)	–
2—CV_702	70 °C, air flow 2 m/s (effective 0.4 m/s)	–
3—CVUD_502200	50 °C, air flow 2 m/s (effective 0.4 m/s)	200 W
4—CVUD_702200	70 °C, air flow 2 m/s (effective 0.4 m/s)	200 W

The tests for all drying schemes were carried out in triplicate. The initial moisture contents of the investigated samples were determined using a Precisa XM120 moisture analyzer, and through drying at 70 °C for 24 h in the chamber drier. The initial moisture content for carrots was equal to 0.88 ± 0.005 kg/kg$_{wb}$, whereas for apples, it was 0.83 ± 0.01kg/kg$_{wb}$. The drying processes were performed until the final moisture content of the carrots reached 0.05 kg/kg$_{wb}$ and that of the apples reached 0.1 kg/kg$_{wb}$. During drying tests, the controller maintained the set process parameters, and collected all the data in its internal memory at constant time intervals. Only the material's temperature was measured independently using a Dwyer HTDL-30 wireless temperature data logger, which allowed the collection of this parameter for material placed in a rotating drum. The wireless Dwyer sensor is a small electronic tube which ends with an elastic thermocouple. The setup was placed

in a drier drum where the thermocouple was placed inside the samples in its center. The sample was secured against slipping from thermocouple by a very thin string.

Figure 3 shows the drying kinetics, i.e., the drying curves and the curves of temperature evolution, obtained experimentally. It is convenient to analyze the drying kinetics with the use of temperature curves. The drying kinetics of both materials show the presence of a heating period for the material, the absence of the first drying period (no constant temperature), and the presence of a second drying period. The drying kinetics of apples shows the existence of the single FDRP curve. In contrast, the carrot kinetics, especially the change in the temperature rise rate, indicates the existence of two stages of the FDRP curves.

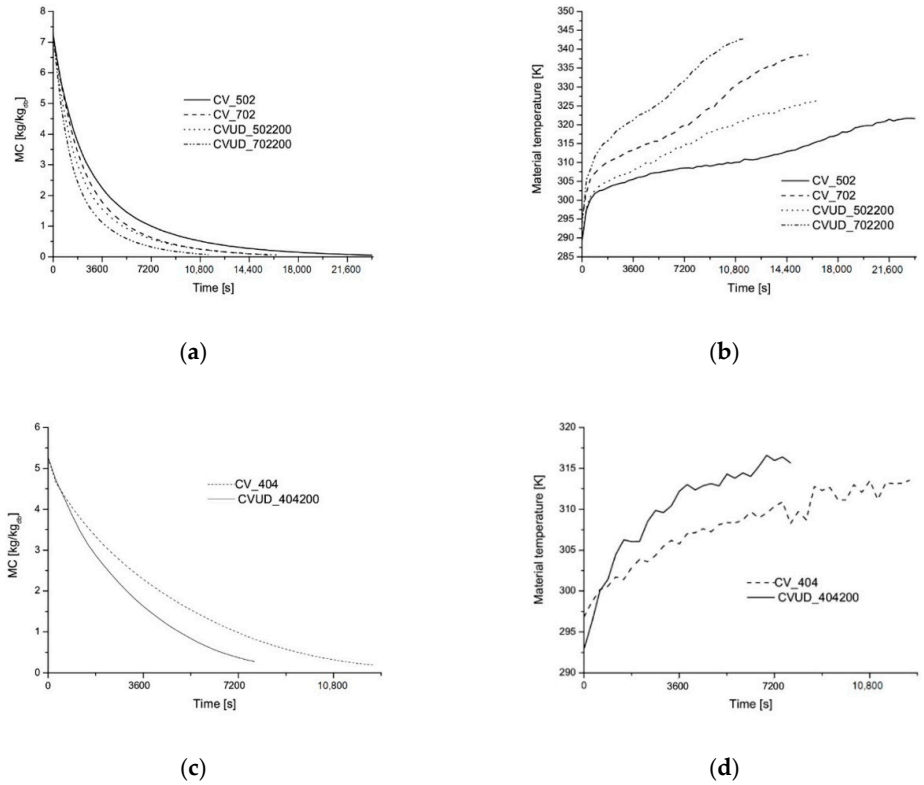

Figure 3. Drying kinetics of the ultrasound-assisted convective drying of carrot samples: (**a**) Drying curves and (**b**) temperature evolution curves. Drying kinetics of the ultrasound-assisted convective drying of apple samples: (**c**) Drying curves and (**d**) temperature evolution curves.

The temperature of the drying medium, T_a, was about 40, 50, and 70 °C. When ultrasound was applied in drying schemes CVUD_404200, CVUD_502200, and CVUD_702200, the material temperature T increased above the drying medium temperature T_a due to the absorption of ultrasonic waves. This phenomenon follows from the additional heat source ΔQ.

6. Numerical Results

The proposed method of parameter estimation in the drying model was tested using the experimental data described in the previous paragraph. According to the experimental results, all of the processes showed no first drying period. Therefore, the values of the critical moisture content X_{cr} for all drying schemes were assumed to be equal to the initial one X_0.

The drying kinetics of apples did not demonstrate the existence of two stages of the FDRP. Therefore, Equation (5) describing the FDRP was used in the mathematical model.

Unlike the drying kinetics of apples, the drying kinetics of carrots reveals the existence of two stages of the FDRP. Therefore, Equation (6) describing these two stages was used in the mathematical

model. The values of the second critical moisture content X_{cr2} were estimated on the basis of the drying kinetics (experimental data), and are given in Table 2.

Table 2. Results of the model parameters determination for carrot samples.

Scheme No. and Abbreviation	Calculated Parameters				Assumed Value	Value of the Objective Function
	h_m (kg/m^{2}s)	h_T (J/m^{2}sK)	φ_{cr2} (1)	ΔQ (W)	X_{cr2} (kg/kg)	$f(h_m,h_T,\Delta Q,\varphi_{cr2})$
1—CV_502	0.000416	24.3	0.191	–	0.3	0.6589
2—CV_702	0.00116	20.8	0.194	–	1.0	0.2682
3—CVUD_502200	0.000773	44.5	0.323	0.584	0.3	0.1048
4—CVUD_702200	0.00140	40.5	0.275	0.887	0.8	0.1219

The Rosenbrock optimization scheme was applied for the determination of the model parameters. The method requires a starting point in the optimization variable space. The optimization method is considered to be convergent if it gives the same result, regardless of the assumed starting point. Therefore, all calculations were carried out using different starting points for the optimization procedure (h_m, h_T, φ_{cr}, and ΔQ). Examples of optimization procedure paths are shown in Figure 4. The chart shows three optimization paths (red, blue, and green). Each of these paths starts at a different point in space (points 1, 2, and 3 in Figure 4). For clarity, the chart was made with the standardized variable ranging from zero to the maximum value occurring during the calculation. Each of these paths was obtained as a result of the optimization procedure starting from a different point in the optimization variable space. It was found, regardless of the starting point of the performed calculations, that the same optimal point was obtained (see Figure 4). This means that the objective function, f, had only one minimum, and that the proposed algorithm was convergent to this solution.

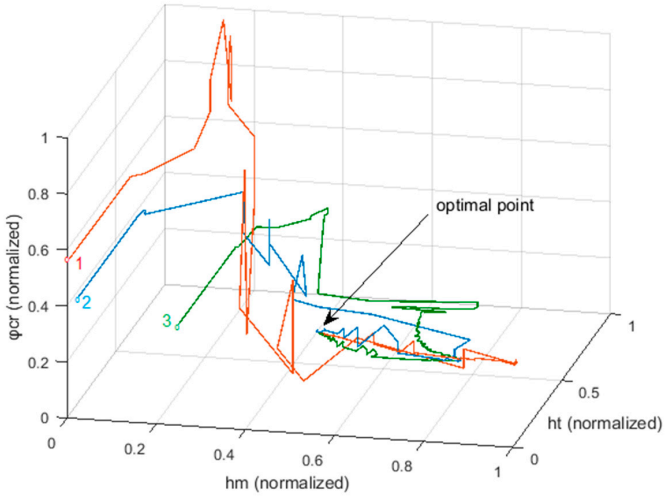

Figure 4. Optimization paths of the mass and heat transfer coefficients and the critical relative humidity (h_m, h_T, and φ_{cr}) (drying scheme CVUD_502200).

The numerical procedure was used to calculate process parameters describing the heat and mass transfer during all of the performed experimental tests. Examples of the drying kinetics obtained, both during experiments and by numerical simulations, are shown in Figure 5. The results demonstrate a good qualitative and quantitative agreement between the experimental and numerical results. It should be noted that the proposed procedure involves two tasks. The first concerns solving nonlinear equations for long-term integration of the model equations. The second is the search for the optimal solution. The performed tests exhibited a good convergence of both tasks, namely, of the initial problem solution and the optimization method.

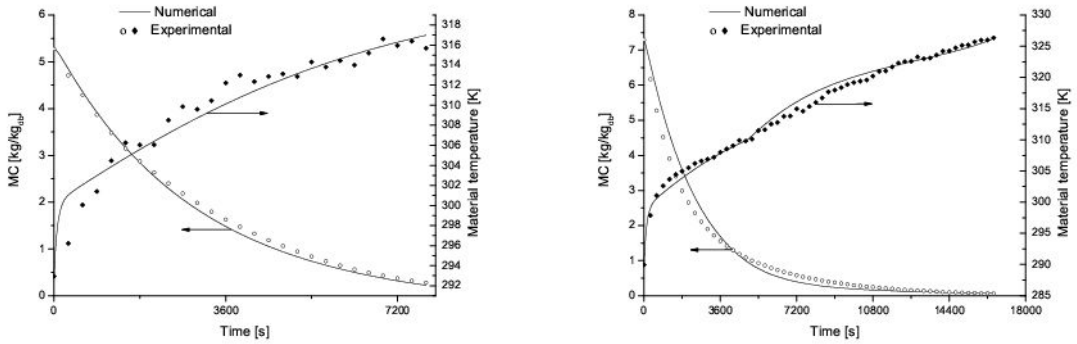

Figure 5. Drying kinetics of ultrasound-assisted convective drying: (**a**) Drying of apple—drying scheme CVUD_404200, and (**b**) drying of carrot—drying scheme CVUD_502200.

Tables 2 and 3 summarize the results of the presented studies. The parameters, which describe the drying process, namely, the effective coefficients of heat h_T and mass h_m convective transfer, the additional heat source ΔQ, and the critical relative humidity φ_{cr2}, were determined using the optimization procedure described previously (in the section on the estimation of model parameters). It was found that ultrasound application improves all parameters (h_m, h_T, and φ_{cr2}) describing the convective heat and mass transfer between the samples and the drying medium. It was also found that the heating effect of ultrasound application caused by the ultrasound's absorption ΔQ was very small. The power of the energy absorbed was less than 1% of the ultrasound generator's power.

Table 3. Results of the model parameter determination for apple samples.

Scheme No. and Abbreviation	Calculated Parameters			Value of the Objective Function $f(h_m,h_T,\Delta Q,X_{cr})$
	h_m (kg/m^{2}s)	h_T (J/m^{2}sK)	ΔQ (W)	
1—CV_404	0.000501	22.5	–	0.1235
2—CVUD_404200	0.000843	29.4	0.158	0.1321

7. Discussion

The described method has been used by the authors to determine the coefficient of the mass transfer of strawberries [35], raspberries [36], and green pepper [37]. The mass transfer coefficient in the case of convective drying was equal to 8.61×10^{-5}, 1.73×10^{-4}, and 2.80×10^{-4} kg/m^2 s, for the strawberries, raspberries, and green pepper, respectively. The application of ultrasound resulted in an increase of the coefficient by 96% for the strawberries, 45% for the raspberries, and 26% for the green pepper. These results indicate that the mass transfer coefficient depends on the material to be dried. The values of the coefficient of the mass transfer obtained in the present work presented in Tables 2 and 3 are an order of greater value. This results from the differences in the movement of the material in the dryer. The pouring of the material in rotating cylinder construction improves the heat and mass transfer. The obtained results show that both estimated transfer coefficients depend on the material to be dried, the dryer construction, and the drying conditions.

8. Conclusions

In this article, an optimization procedure is proposed for determination of the coefficient in the drying model used by the authors. The coefficients of the effective heat and mass transfer by convective drying and convective drying enhanced with ultrasound are introduced. The presented drying model and the method of coefficient estimation enable the description of the single stage of the falling drying

period (FDRP) (drying of apples) and two stages of the falling drying rate period (FDRP) (drying of carrots) for the drying processes of bio-products. The performed tests showed a good convergence of the solution and the optimization methods. The good quality of the solution was confirmed by the compliance of the model results with the experimental results (Figure 5). The application of the Adams–Bashforth method resulted in solution compatibility, especially in the part describing the transition between the drying periods and in the part of the solution describing the end of the process. The good quality of the applied optimization scheme was confirmed by the convergence of the solution at one point, regardless of the starting point in the variable space (Figure 4). The quality of both the equation solving procedure and the optimization procedure was quantified by the low value of the objective function (Tables 2 and 3).

The kinetic parameters determined from the numerical calculation showed the positive influence of convective drying with ultrasound enhancement for both tested materials. The results of the performed calculations confirm that absorption of the air-borne ultrasound energy into the dried material is very small. The method presented in this article was shown to be very efficient for determination of the heat and mass transfer processes based on the presented model of drying kinetics. This model could be easily extended to other complex drying processes, for example, hybrid drying based on several drying techniques.

Author Contributions: Conceptualization, G.M. and M.S.; methodology, G.M. and M.S.; software preparation, M.S.; experiments D.M.; numerical calculation, M.S.; results visualization D.M. and M.S.; writing—original draft preparation, G.M.; writing—review and editing, M.S., G.M., and D.M. All authors have read and agreed to the published version of the manuscript.

Funding: This work was supported by the Polish Ministry of Science and Higher Education.

Conflicts of Interest: The authors declare no conflict of interest.

Nomenclature

Symbol	Designation	Unit
c_s	specific heat of dry solid	J/kgK
c_l	specific heat of moisture (water)	J/kgK
f	objective function	1
h_m	mass transfer coefficient	kg/m^{2}s
h_T	heat transfer coefficient	J/m^{2}sK
l	latent heat of evaporation	J/kg
m_s	dry mass	kg
p_{vs}	saturated vapor pressure	Pa
t	time	s
A	surface of sample	m^2
A_0	initial surface of sample	m^2
A_m	surface of mass exchange	m^2
A_T	surface of heat exchange	m^2
MC	moisture content dry basis	kg/kg$_{db}$
T	absolute temperature	K
T_0	initial temperature	K
T_a	ambient air temperature	K
T_{exp}	experimental value of temperature	K
T_{max}	maximal value of temperature	K
T_{min}	minimal value of temperature	K
T_{num}	numerical value of temperature	K
V	volume of sample	m^3
V_0	initial volume of sample	m^3

X	moisture content dry basis	kg/kg_{db}
X_0	initial moisture content dry basis	kg/kg_{db}
X_{cr}	critical moisture content dry basis	kg/kg_{db}
X_{cr2}	second critical moisture content dry basis	kg/kg_{db}
X_{eq}	equilibrium moisture content dry basis	kg/kg_{db}
X_{exp}	experimental value of moisture content	kg/kg_{db}
X_{max}	maximal value of moisture content	kg/kg_{db}
X_{min}	minimal value of moisture content	kg/kg_{db}
X_{num}	numerical value of moisture content	kg/kg_{db}
α_V	volumetric shrinkage coefficient	1
φ	relative air humidity	1
φ_a	relative air humidity in ambient air	1
$\varphi\big\vert_{\partial B}$	air humidity close to the dried sample surface	1
φ_{cr2}	second critical air relative humidity	1
ΔQ	heat due to absorption of ultrasonic waves	W
$\Phi(t, X, t)$	function—simplifying designation	kg/s
$\Psi(t, X, t)$	function—simplifying designation	K/s

References

1. Jayaraman, K.S.; Das Gupta, D.K. Drying of Fuits and Vegetables. In *Handbook of Industrial Drying*, 4th ed.; Mujumdar, A.S., Ed.; CRC Press: Boca Raton, FL, USA, 2014; pp. 611–636.
2. Chen, G.; Mujumdar, A.S. Drying Herbal Medicines and Tea. In *Handbook of Industrial Drying*, 4th ed.; Mujumdar, A.S., Ed.; CRC Press: Boca Raton, FL, USA, 2014; pp. 637–646.
3. Musielak, G.; Mierzwa, D.; Kroehnke, J. Food Drying Enhancement by Ultrasound—A Review. *Trends Food Sci. Technol.* **2016**, *56*, 126–141. [CrossRef]
4. Szadzińska, J.; Pashminehazar, R.; Kharaghani, A.; Tsotsas, E.; Łechtańska, J. Microwave and Ultrasound Assisted Convective Drying of Raspberries: Drying Kinetics and Microstructural Changes. *Dry. Technol.* **2018**, *37*, 1–12. [CrossRef]
5. Gallego-Juárez, J.A.; Riera, E.; de la Fuente Blanco, S.; Rodriguez-Corral, G.; Acosta-Aparicio, V.M.; Blanco, A. Application of High-Power Ultrasound for Dehydration of Vegetables: Processes and Devices. *Dry Technol.* **2007**, *25*, 1893–1901. [CrossRef]
6. Cárcel, J.A.; García-Pérez, J.V.; Benedito, J.; Mulet, A. Food Process Innovation through New Technologies. *J. Food Eng.* **2012**, *110*, 200–207. [CrossRef]
7. Bantle, M.; Hanssler, J. Ultrasonic Convective Drying Kinetics of Clipfish during the Initial Drying Period. *Dry Technol.* **2013**, *31*, 1307–1316. [CrossRef]
8. Siucińska, K.; Konopacka, D. Application of Ultrasound to Modify and Improve Dried Fruit and Vegetable Tissue—A Review. *Dry Technol.* **2014**, *32*, 1360–1368. [CrossRef]
9. Kowalski, S.J.; Mierzwa, D. Ultrasound-Assisted Convective Drying of Biological Materials. *Dry Technol.* **2015**, *33*, 1601–1613. [CrossRef]
10. Kowalski, S.J.; Pawłowski, A. Intensification of Apple Drying due to Ultrasound Enhancement. *J. Food Eng.* **2015**, *156*, 1–9. [CrossRef]
11. Gallego-Juárez, J.A.; Rodríguez-Corral, G.; San Emeterio-Prieto, J.L.; Montoya-Vitini, F. Electroacoustic Unit for Generating High Sonic and Ultrasonic Intensities in Gases and Interphases. U.S. Patent No. 5,299,175, 29 March 1994.
12. Gallego-Juárez, J.A.; Riera, E.; Rodríguez-Corral, G.; Gálvez Moraleda, J.C.; Yang, T.S. A New High-Intensity Ultrasonic Technology for Food Dehydration. *Dry Technol.* **1999**, *17*, 597–608. [CrossRef]
13. García-Pérez, J.V.; Cárcel, J.A.; de la Fuente-Blanco, S.; Riera-Franco de Sarabia, E. Ultrasonic Drying of Foodstuff in a Fluidized Bed: Parametric Study. *Ultrasonics* **2006**, *44*, e539–e543. [CrossRef]
14. Khmelev, V.N.; Shalunov, A.V.; Barsukov, R.V.; Abramenko, D.S.; Lebedev, A.N. Studies of Ultrasonic Dehydration Efficiency. *J. Zhejiang Univ. Sci. A* **2011**, *12*, 247–254. [CrossRef]
15. Kouchakzadeh, A.; Ghobadi, P. Modeling of Ultrasonic-Convective Drying of Pistachios. *Agric. Eng. Int. CIGR J.* **2012**, *14*, 144–149.

16. Konopacka, D.; Parosa, R.; Piecko, J.; Połubok, A.; Siucińska, K. Ultrasound & Microwave Hybrid Drying Device for Colored Fruit Preservation—Product Quality and Energy Efficiency. In Proceedings of the 8th Asia-Pacific Drying Conference (ADC 2015), Kuala Lumpur, Malaysia, 10–12 August 2015; pp. 252–258.
17. Cárcel, J.A.; García-Pérez, J.V.; Riera, E.; Mulet, A. Influence of Highintensity Ultrasound on Drying Kinetics of Persimmon. *Dry Technol.* **2007**, *25*, 185–193. [CrossRef]
18. García- Pérez, J.V.; Cárcel, J.A.; Benedito, J.; Mulet, A. Power Ultrasound Mass Transfer Enhancement in Food Drying. *Food Bioprod. Process.* **2007**, *85*, 247–254. [CrossRef]
19. Cárcel, J.A.; García-Pérez, J.V.; Riera, E.; Mulet, A. Improvement of Convective Drying of Carrot by Applying Power Ultrasound. Influence of Mass Load Density. *Dry Technol.* **2011**, *29*, 174–182. [CrossRef]
20. Gamboa-Santos, J.; Montilla, A.; Cárcel, J.A.; Villamiel, M.; García-Pérez, J.V. Air-Borne Ultrasound Application in the Convective Drying of Strawberry. *J. Food Eng.* **2014**, *128*, 132–139. [CrossRef]
21. Rodríguez, O.; Santacatalina, J.V.; Simal, S.; García- Pérez, J.V.; Femenia, A.; Rosselló, C. Influence of Power Ultrasound Application on Drying Kinetics of Apple and its Antioxidant and Microstructural Properties. *J. Food Eng.* **2014**, *129*, 21–29. [CrossRef]
22. Kowalski, S.J.; Pawłowski, A. Modeling of Kinetics in Stationary and Intermittent Drying. *Dry Technol.* **2010**, *28*, 1023–1031. [CrossRef]
23. Aversa, M.; Van der Voort, A.-J.; de Heij, W.; Tournois, B.; Curcio, S. An Experimental Analysis of Acoustic Drying of Carrots: Evaluation of Heat Transfer Coefficients in Different Drying Conditions. *Dry Technol.* **2011**, *29*, 239–244. [CrossRef]
24. Raszkowski, T.; Samson, A. Numerical Approaches to the Heat Transfer Problem in Modern Electronic Structures. *Comput. Sci.* **2017**, *18*, 71–93. [CrossRef]
25. Zwarycz-Makkles, K.; Majorkowska-Mech, D. Gear and Runge-Kutta Numerical Discretization Method in Differential Equations of Adsorption in Adsorption Heat Pump. *Appl. Sci.* **2018**, *8*, 2437. [CrossRef]
26. Duc, L.A.; Hyuk, K.D. Mathematical Modeling and Simulation of Rapeseed Drying on Concurrent-Flow Dryer. In *Current Drying Processes*; Palqa-Rosas, I., Ed.; IntechOpen: Rijeka, Croatia; London, UK, 2020. [CrossRef]
27. Krupowicz, A. *Numerical Methods of Initial Value Problems of Ordinary Differential Equations*; PWN: Warsaw, Poland, 1986.
28. Rosenbrock, H.H. An Automatic Method for Finding the Greatest or Least Value of a Function. *Comput. J.* **1960**, *3*, 175–184. [CrossRef]
29. Mujumdar, A.S. Principles, Classification, and Selection of Dryers. In *Handbook of Industrial Drying*, 4th ed.; Mujumdar, A.S., Ed.; CRC Press: Boca Raton, FL, USA, 2014; pp. 3–30.
30. Musielak, G.; Banaszak, J. Non-Linear Heat and Mass Transfer during Convective Drying of Kaolin Cylinder under Non-Steady Conditions. *Transp. Porous Media* **2007**, *66*, 121–134.
31. Strumiłło, C. *Foundations of the Drying Theory and Technology*, 2nd ed.; WNT: Warsaw, Poland, 1983.
32. Davis, M. *Numerical Methods and Modelling for Chemical Engineers*; Wiley: Montreal, QC, Canada, 1984.
33. Toledo, R.T. *Fundamentals of Food Process Engineering*; Heldman, D.R., Ed.; Springer: New York, NY, USA, 2007.
34. DTU Food. Available online: http://www.foodcomp.dk/v7/fcdb_details.asp?FoodId=1128 (accessed on 16 April 2016).
35. Szadzińska, J.; Kowalski, S.J.; Stasiak, M. Microwave and ultrasound enhancement of convective drying of strawberries: Experimental and modeling efficiency. *Int. J. Heat Mass Transf.* **2016**, *103*, 1065–1074. [CrossRef]
36. Kowalski, S.J.; Pawłowski, A.; Szadzińska, J.; Łechtańska, J.; Stasiak, M. High power airborne ultrasound assist in combined drying of raspberries. *Innov. Food Sci. Emerg. Technol.* **2016**, *34*, 225–233. [CrossRef]
37. Szadzińska, J.; Łechtańska, J.; Kowalski, S.J.; Stasiak, M. The effect of high power airborne ultrasound and microwaves on convective drying effectiveness and quality of green pepper. *Ultrason. Sonochem.* **2017**, *34*, 531–539. [CrossRef]